European Conference on Optical Communication (ECOC) 2022 © Optica Publishing Group 2022

Spatially Disaggregated Modelling of Self-Channel NLI in Mixed Fibers Optical Transmission

Emanuele Virgillito(1), Andrea Castoldi(2), Andrea D'Amico(1), Stefano Straullu(3), Rudi Bratovich(2), Fransisco M. Rodriguez (2), Andrea Bovio (2), Rosanna Pastorelli(2), Vittorio Curri(1)

(1) Politecnico di Torino, Italy emanuele.virgillito@polito.it (2) SM-Optics, Italy (3) LINKS Foundation, Italy

Abstract *We simulate and observe the buildup of coherency in self-channel interference. We propose a spatially disaggregated model for non-uniform links with uncompensated and compensated spans. We show that the correlation coefficient can be described by a unique curve. ©2022 The Author(s)*

Introduction

Dual-Polarization (DP) coherent transmission technology at 100Gbps+ dominates the backbone network market made up of fiber links without dispersion compensation units (DCU). On the contrary, the metro and access network segment still largely employs legacy intensity modulated, direct detected (IMDD) channels delivering 10 Gbps on dispersion managed (DM) optical line systems (OLS). Thus, in these network segments we see a progressive deployment of coherent optical technologies co-existing with IMDD and so propagating on DM OLSs. It has been shown that nonlinear propagation of DP coherent technologies is well modeled with the nonlinear interference (NLI), whose main components are the self- (SCI) and cross- (XCI) channel interference induced by the channel on itself and by co-propagating coherent[1] or IMDD channels[2], respectively. The physical mechanisms allow a disaggregated approach[3] to the NLI evaluation, also in mixed fibers scenarios[4], in uncompensated transmission (UT) lines. In case of DM OLS with limited residual dispersion per span the disaggregated approach may hold, but due to its statistical coherent accumulation, the effect of SCI may be severe. Also, SCI becomes predominant w.r.t. XCI with the evolution towards ultra-high symbol rates R_s. Moreover, network architectures are evolving towards the openness and disaggregation[3],[5],[6], so a disaggregated NLI evaluation is needed in mixed fiber and DM OLS also for the SCI. In this work, we observe by split-step Fourier method (SSFM) simulations the accumulation of the SCI in mixed-fiber DM lines. We show that the overall SCI over a DM mixed line can be be computed considering the *pure* (intrinsic) SCI per span that is conservatively given by the incoherent GN (IGN)[7] model, then each contribution is added up considering the coherency coefficients. We show that the correlation coefficients depend on a generic law that applies to all considered systems and depends on two parameters: the amount of dispersion in R_s accumulated between two spans that increases the decorrelation and the amount of dispersion in R_s accumulated by each span in the effective length that reduces the decorrelation.

Modeling and Simulation of SCI Coherency

We need an adequate system model for a spatially disaggregated estimation of the SCI coherency on non-uniform, realistic link. We consider an OLS as in Fig.1 (up), accounting for non-uniform fiber spans with different physical parameters. Although we operate the OLSs in trasparency, so that $A_i G_i = 1$, this assumption may be relaxed without loss of generality. To include segments of DM links, each span may be also equipped with a DCU setting the residual dispersion $D_{RES} = DL_s + D_{DCU}$ (being D and L_s the fiber dispersion coefficient and length), depending on the 10G dispersion map. UT is obtained setting $D_{DCU} = 0$ ps/nm, so that $D_{RES} = DL_s$ ps/nm. Our modeling is based on the abstraction in the Fig.1 (down) diagram, where each span is modeled as a spatially disaggregated entity introducing a *pure* SCI random process $n_i(t)$. As long as the span length exceeds the fiber's effective length, the SCI can be equivalently modeled as a lumped additive noise at the beginning of the fiber[7],[8]. Consequently, this pure SCI component is assumed independent on the subsequent dispersion contributions. However it has been argued that the degree of coherency[7],[9]–[11] depends on the following amount of dispersion experieced through the OLS. This makes the overall SCI estimation not anymore memoryless but propagation history dependent. This memory effect is modeled by introducing a multiplicative, complex coefficient d_i, related to the accumulated phase due to the i-th span dispersion, including

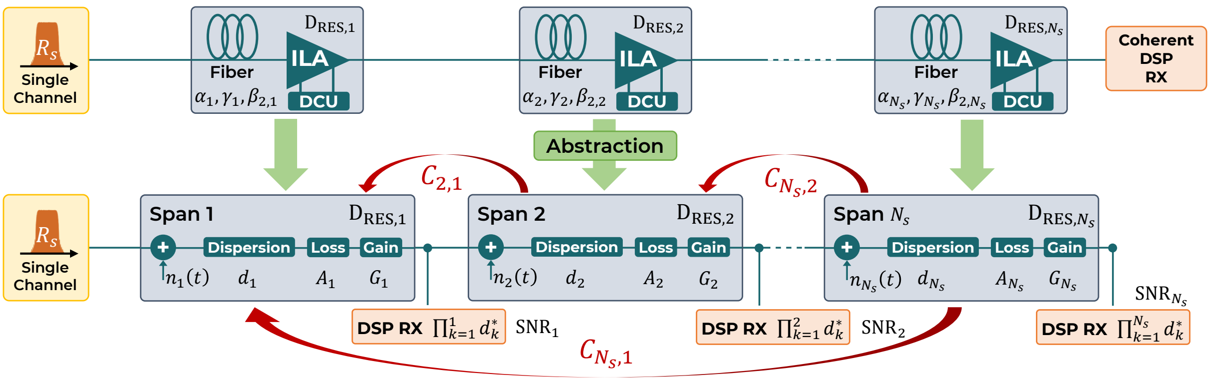

Fig. 1: The considered optical system (up) and its system abstraction (down), in general non-uniform and non-periodic. In simulation we receive at the end of all the spans to obtain the SNR accumulation.

the DCU[9]. The $n_i(t)$ contribution is then propagated throughout the rest of the link, so that it undergoes the subsequent dispersion, including the final, opposite contribution due to chromatic dispersion compensation (CDC). Hence, the overall noise field after k spans ($k = 1 \dots N_s$), CDC, equalizer and CPE is $\hat{n}_k(t) = \sum_{i=1}^{k} n_i(t) \prod_{j=1}^{i-1} d_j^*$ We then calculate the amount of coherent SCI noise introduced by the i-th span as the accumulated noise powers difference between two adjacent spans $\Delta P_{SCI,i} = P_{SCI,i} - P_{SCI,i-1} = E[|\hat{n}_i(t)|^2] - E[|\hat{n}_{i-1}(t)|^2]$, being $E[\cdot]$ the statistical average operator. Due to the statistical dependence between the *pure* SCI terms $n_i(t)$, the cross-span terms of the average cannot be neglected, so that, at i-th span:

$$\Delta P_{SCI,i} = \sigma_i^2 + 2 \sum_{j=1}^{i-1} C_{ij} \sigma_i \sigma_j \quad (1)$$

where $\sigma_i^2 = E[|n_i(t)|^2]$ is the power of the *pure* SCI term, dependent on the i-th fiber dispersion coefficient. Each term of the sum instead represent the additional power due to the correlation of the i-th span with each of the preceding. The coefficient C_{ij} is bounded in $[0, 1]$ and weights each of these terms, being related to the product $\prod_{k=j}^{i-1} d_k^*$, i.e. to the previous accumulated dispersion between spans j and $i-1$, thus to the sum of their inline residuals . To validate this model we carried out an extensive simulation

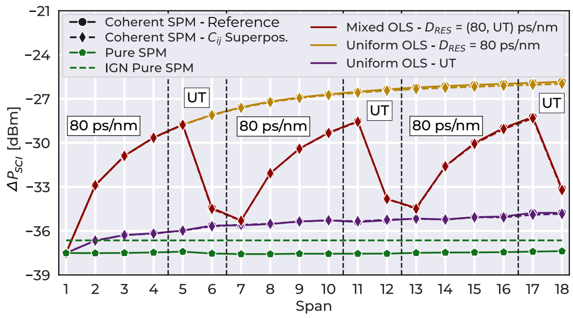

Fig. 2: The ΔP_{SCI} added by each span on uniform and non-uniform OLSs obtained by Full SSFM (circles) and spatial superposition (diamonds).

campaign using the SSFM, propagating a single coherent channel DP-QPSK modulated at symbol rates R_s of 32 and 64 GBaud on a $N_s = 18$ spans OLS. We applied a large amount of predistortion (102400 ps/nm) in order to isolate the coherency effect and avoid the transient due to the signal *gaussianization*[12],[13], which can be considered a separate effect w.r.t. coherency, being a worst-case for the *pure* SCI power σ_i^2. The ILAs have been simulated as ideal (without ASE noise) to isolate the SCI noise power. We receive the signal at each span end by means of a standard DSP based coherent receiver which first applies CDC, determined by the $D_{RES,i}$ up to the point of reception. Then an adaptive equalizer and a carrier phase estimation stage are applied before measuring the SNR. From the curve of the accumulated SNR_i, ($i = 1 \dots N_s$), we extrapolate the SCI power buildup $P_{SCI,i}$ and the corresponding amount of *coherent* SCI noise power introduced by i-th span $\Delta P_{SCI,i}$. On the OLS configuration side, for each R_s, we simulated uniform and non-uniform OLSs. Both cases share the same length $L_s = 80$ km, loss coefficient $\alpha = 0.2$ dB/km, nonlinear coefficient $\gamma = 1.27$ 1/W/km and two possible dispersion coefficients $D = (4, 16)$ ps/nm/km. For each D value, two DM setups with $D_{RES} = 40$ and 80 ps/nm plus the UT have been considered as uniform OLSs. In the non-uniform configurations we have considered spans with mixed residuals $D_{RES,i}$, but keeping the dispersion coefficient constant within the same OLS. We have simulated, for each R_s and D, two residual pairs $D_{RES} = (40, 80)$ ps/nm and $D_{RES} = (80, \mathrm{UT})$ ps/nm: for each pair, the link is composed as the three-fold repetition of a 6x spans module, where the first 4 spans have D_{RES} equal to the pair's first value, while the remaining 2 to the second. Such simulations represent our *reference* scenario illustrating the aggregated effect of pure

SCI and coherency terms. They are reported in Fig.2 with circle markers for the sample mixed residual case of $D_{RES} = (80, \mathrm{UT})$ ps/nm, $D = 16$ ps/nm/km, $R_s = 64$ GBaud, together with the corresponding uniform configuration. In the mixed curve, the first UT span of each module still carries a large coherency due to the small dispersion accumulated by the preceding compensated span. Oppositely, the first compensated span of the 2nd module shows small coherency, because the previous UT span accumulates large dispersion. To test the coherency contributions spatial superposition, for each line configuration, we did another simulation set to isolate the pure σ_i^2 and the C_{ij} terms. The pure term σ_i^2 is obtained by *turning off* the Kerr effect ($\gamma = 0$) in all the spans but the i-th. The resulting green curve (pentagons) in Fig.2 shows that the *pure* SCI is constant independently on the D_{RES} set by the DCU and it is also well-estimated by the IGN model[7]. Similarly, the C_{ij} are obtained with simulations where all the spans but the i-th and j-th have $\gamma = 0$. This allows to isolate a single coherency power term between spans (i, j) and extract the C_{ij} from Eq.1. The overall $\Delta P_{SCI,i}$ reconstructed by spatial superposition of the so obtained C_{ij}, σ_i^2 using Eq.1, is reported in Fig.2 with diamond markers, for both mixed and uniform configurations. They well match the reference simulations with all $\gamma \neq 0$, thus confirming the validity of our approach.

The Coherency Scaling Law

Fig.2 shows that the SCI coherence maybe significant for long links, especially if DM segments are crossed, adding several dB of coherency power. Such non negligible weight poses an important networking problem because a path computation engine must know the entire crossed path to estimate the actual SNR or just a worst-case. At the same time, during path computation the complete path is always known by definition. Hence, it is crucial to elaborate a (semi-)analytical model of the C_{ij} to know their scaling laws with the system parameter. In[10] we observed the behavior of the *cumulative* correlation (i.e. aggregating all the span pair contributions) for UT, uniform links. It turned out to be a decreasing function of the variable θ_{span}, summarizing the propagation phase characteristics, being dependent on the cumulated dispersion and R_s. We apply here the same reasoning for each span pair (i, j), also including DM spans, which enables us to observe the scaling laws at small accumulated dispersion. In Fig.3 we plot the C_{ij} values from all the considered combinations of R_s, D and D_{RES} of mixed and uniform configuration vs the $\theta_{span}(i,j) = R_s^2 \pi \sum_{k=j}^{i-1} (\beta_{2,k} L_s + \beta_{DCU,k})$. Hence, the θ_{span} depends on R_s and the D_{RES} up to the span $i-1$ The plot shows that the C_{ij} decay with the θ_{span} as expected, but with curves grouped in three families. Hence, θ_{span} does not exhaust the coherency features. Indeed, we notice that the families are labelled by the product $R_s^2 D$: in fact, the $R_s = 32$ GBaud, $D = 16$ ps/nm/km and $R_s = 64$ GBaud, $D = 4$ ps/nm/km curves, having constant $R_s^2 D$, are superimposed. Also, visual inspection of Fig.3 suggest that the families are related by a different x-axis compression. We argue that the missing term, apart from θ_{span}, is related to the parameter $\theta_{fiber}(i) = R_s^2 \beta_{2,i} L_{eff,i}$, introducing a C_{ij} dependency on the i-th fiber parameters. Fig.4 shows that rescaling the x-axis to the variable ${}^{\theta_{span}(i,j)}/_{\sqrt{\theta_{fiber}(i)}}$ indeed makes the three groups to merge into a single one.

Conclusion

With SSFM simulations we found a unique curve describing the degree of SCI coherency in a spatially disaggregated way, which can be used in network control and design tools to assess the overall SCI power by labelling the link with their $\theta_{span}(i, j)$ and $\theta_{fiber}(i)$ parameters, even in a non-uniform links scenario. Further works will focus on the validation with non-uniform loss and dispersion coefficients.

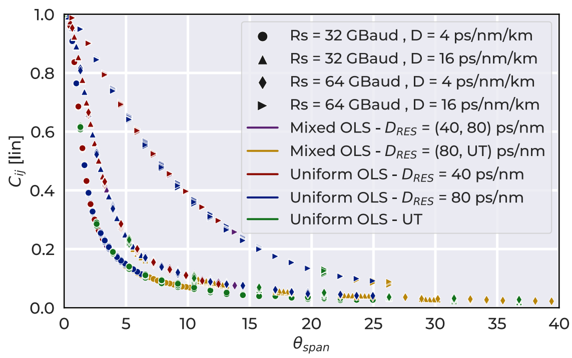

Fig. 3: The C_{ij} vs $\theta_{span}(i, j)$ as in[10] for all the scenarios

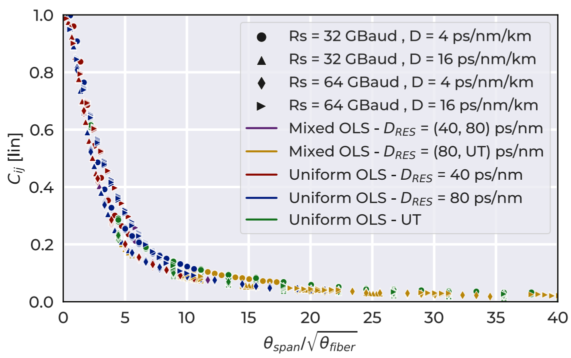

Fig. 4: The C_{ij} vs ${}^{\theta_{span}(i,j)}/_{\sqrt{\theta_{fiber}(i)}}$ for all the scenarios

References

[1] A. Bononi, O. Beucher, and P. Serena, "Single- and cross-channel nonlinear interference in the gaussian noise model with rectangular spectra", *Opt. Express*, vol. 21, no. 26, pp. 32 254–32 268, Dec. 2013.

[2] E. Virgillito, A. Castoldi, S. Straullu, R. Pastorelli, and V. Curri, "Qot computation for 100g lightpaths routed on 10g-loaded dispersion-managed network segments", in *2021 International Conference on Electrical, Communication, and Computer Engineering (ICECCE)*, 2021, pp. 1–6. DOI: 10.1109/ICECCE52056.2021.9514126.

[3] V. Curri, "GNPy model of the physical layer for open and disaggregated optical networking [invited]", *J. Opt. Commun. Netw.*, vol. 14, no. 6, pp. C92–C104, Jun. 2022.

[4] E. London, A. D'Amico, E. Virgillito, A. Napoli, and V. Curri, "Modelling non-linear interference in non-periodic and disaggregated optical network segments", *Opt. Continuum*, vol. 1, no. 4, pp. 793–803, Apr. 2022.

[5] M. Birk, O. Renais, G. Lambert, *et al.*, "The openroadm initiative [invited]", *J. Opt. Commun. Netw.*, vol. 12, no. 6, pp. C58–C67, Jun. 2020. DOI: 10.1364/JOCN.380723. [Online]. Available: http://opg.optica.org/jocn/abstract.cfm?URI=jocn-12-6-C58.

[6] R. Casellas, R. MartÃnez, R. Vilalta, and R. MuÃ$\pm oz$, "Abstraction and control of multi-domain disaggregated optical networks with openroadm device models", *Journal of Lightwave Technology*, vol. 38, no. 9, pp. 2606–2615, 2020. DOI: 10.1109/JLT.2020.2969248.

[7] P. Poggiolini, "The gn model of non-linear propagation in uncompensated coherent optical systems", *Journal of Lightwave Technology*, vol. 30, no. 24, pp. 3857–3879, 2012. DOI: 10.1109/JLT.2012.2217729.

[8] A. Carena, V. Curri, G. Bosco, P. Poggiolini, and F. Forghieri, "Modeling of the impact of nonlinear propagation effects in uncompensated optical coherent transmission links", *J. of Lightwave Tech.*, vol. 30, no. 10, pp. 1524–1539, May 2012. DOI: 10.1109/jlt.2012.2189198.

[9] P. Poggiolini, G. Bosco, A. Carena, V. Curri, Y. Jiang, and F. Forghieri, *A detailed analytical derivation of the gn model of non-linear interference in coherent optical transmission systems*, 2014. arXiv: 1209.0394 [physics.optics].

[10] A. DâAmico, E. London, E. Virgillito, A. Napoli, and V. Curri, "Quality of transmission estimation for planning of disaggregated optical networks", in *2020 International Conference on Optical Network Design and Modeling (ONDM)*, 2020, pp. 1–3. DOI: 10.23919/ONDM48393.2020.9133012.

[11] P. Serena and A. Bononi, "An alternative approach to the gaussian noise model and its system implications", *Journal of Lightwave Technology*, vol. 31, no. 22, pp. 3489–3499, 2013. DOI: 10.1109/JLT.2013.2284499.

[12] P. Poggiolini, G. Bosco, A. Carena, V. Curri, Y. Jiang, and F. Forghieri, "A simple and effective closed-form gn model correction formula accounting for signal non-gaussian distribution", *Journal of Lightwave Technology*, vol. 33, no. 2, pp. 459–473, 2015. DOI: 10.1109/JLT.2014.2387891.

[13] P. Poggiolini and Y. Jiang, "Recent advances in the modeling of the impact of nonlinear fiber propagation effects on uncompensated coherent transmission systems", *Journal of Lightwave Technology*, vol. 35, no. 3, pp. 458–480, 2017. DOI: 10.1109/JLT.2016.2613893.